Supporting Information

Controlled crystallinity nano-$Li_{1.2}Cr_{0.4}Mn_{0.4}O_2$ cathode for lithium ion batteries

Ayuko Kitajou[1,*], Shohei Matsuda[1], Koji Ohara[2], Kazutaka Ikeda[3] and Shunsuke Muto[4,5]

[1] Graduate School of Sciences and Technology for Innovation, Yamaguchi University, 2-16-1 Tokiwadai, Ube, Yamaguchi 755-8611, Japan
[2] Faculty of Materials for Energy, Shimane University, 1060, Nishikawatsu-Cho, Matsue, Shimane, 690-8504, Japan
[3] Institute of Materials Structure Science, High Energy Accelerator Research Organization (KEK), Tokai, Ibaraki 319-1106, Japan
[4] Graduate School of Engineering, Nagoya University, Furo-cho, Chikusa-ku, Nagoya, Aichi 464-8603, Japan
[5] Advanced Measurement Technology Center, Institute of Materials and Systems for Sustainability, Nagoya University, Furo-cho, Chikusa-ku, Nagoya, Aichi 464-8603, Japan

* corresponding author
Ayuko Kitajou
E-mail: kitajou@yamaguchi-u.ac.jp

Experimental section

1 Synthesis and electrochemical measurement of the cathode materials

The layered $Li_{1.2}Cr_{0.4}Mn_{0.4}O_2$ (layered-LCMO) was synthesized by the solid-state synthesis method. Stoichiometric amounts of Li_2CO_3, Mn_2O_3, and Cr_2O_3 were mixed and heated at 500 ^oC for 5 h in air and then allowed to cool. The sintered material was mixed, ground, and sintered again at 950 ^oC for 12 h in Ar. The disordered $Li_{1.2}Cr_{0.4}Mn_{0.4}O_2$ (milled-LCMO) was prepared for ball-milling using a planetary mill (Pulverisette7; Fritsch) at 600 rpm for 6 h in air. Here, the layered-LCMO powders (1.5 g) were put in an 80-mlcontainer with ϕ3 mm-ZrO_2 balls (40 g). For the thermal treatment, the milled-LCMO was sintered at 500 ~ 800 ^oC in an Ar atmosphere for 1 h. Here the samples treated in that temperature range are called 500-LCMO, 600-LCMO, 700-LCMO, and 800-LCMO. To obtain uniform carbon composites, the obtained mixtures, consisting of 80 wt.% of each powder and 10 wt.% of acetylene black (AB; Denka Company Ltd.), were subjected to the carbon composite process. This obtained sample and AB were dry ball-milled at 400 rpm for 0.5 h in air. Sheet-type electrodes were prepared by mixing the obtained products, comprising 90 wt% of above carbon composites, 5 wt% of AB, and 5 wt% of a PVDF binder (#7305; Kureha Corp.). Here, the final weight ratio of the obtained sample, AB, and PVDF binder in the electrode was 80 : 15 : 5 wt%. The resulting slurry was coated on aluminum foil and dried at 80 °C for 30 min. The loaded amount of the obtained samples in the sheet-type cathode was ca. 3 mg cm^{-2} (only active materials) in the electrodes. The cathode properties were evaluated using a 2032 coin-type cell assembled in an Ar-filled glove box with a dew point of -80 °C. All cells were assembled using a polypropylene separator (3501, Celgard LLC), lithium metal (Honjo Metal Co.) as the anode material, and a non-aqueous electrolyte composed of 1 M $LiPF_6$/EC:DMC

(1:1 in volume, Tomiyama Pure Chemical Industries, Ltd.) combined with 0.5 M lithium bis(trifluoromethanesulfonyl)imide (LiTFSI, Kanto Chemical Co., Inc.) in N, N-diethyl-N-methyl-N-(2-methoxyethyl) ammonium bis (trifluoro-methanesulfonyl) imide (DEMETFSI, Kanto Chemical Co., Inc.)). The elution amount of Mn and Cr ions in electrolyte was evaluated using inductively coupled plasma atomic emission spectroscopy (ICP-AES).

2 Physical characterization of the obtained samples

Powder X-ray diffraction (XRD) was carried out on a Rigaku Miniflex600 using Cu Kα radiation (40 keV, 15 mA). The X-ray total scattering measurements using synchrotron radiation were carried out with an incident X-ray energy of 61.4 keV at room temperature at beamline BL04B2 of SPring-8, Japan. The obtained powders (layered-LCMO, milled-LCMO, and 600-LCMO) were each sealed in a quartz capillary with a 2 mm inner diameter. The data were collected using Ge and CdTe hybrid detectors. The maximum momentum transfer, Q_{max}, for the measurements was approximately 25 Å^{-1}. The coherent X-ray scattering intensities, $I_{exp}(Q)$, were obtained by subtracting the absorption, the Compton scattering, and the contribution of the quartz capillary from the raw X-ray scattering intensities. The Faber–Ziman structure factor $S(Q)$[1] was obtained by normalizing the $I_{exp}(Q)$. The reduced pair distribution function $G(r)$ was obtained using the conventional Fourier transform of the $S(Q)$[2]. The neutron total scattering measurements were carried out at beamline BL21 (NOVA) of MLF, J-PARC. These samples were sealed in a V-Ni null scattering sample container with an outer diameter of 6.0 mm and a thickness of 0.1 mm and were measured for an exposure time of 5 h at room

temperature. Contamination from the background intensities of the sample container and the instrument was subtracted, and the neutron attenuation factors of the sample and sample container were calibrated to obtain neutron $S(Q)$. The atomic arrangements of the samples were investigated by fitting the diffraction pattern and its Fourier transform as a pair distribution function (PDF) using GSAS-II[3] in conjunction with RMCProfile [4]. We used superlattices with three dimensions 10 × 10 × 2 ($Li_{715}Cr_{242}Mn_{243}O_{1200}$; layered-LCMO), 8 × 8 × 8 ($Li_{1232}Cr_{407}Mn_{409}O_{2048}$; milled-LCMO), and 8 × 8 × 8 ($Li_{1181}Cr_{452}Mn_{415}O_{2048}$; 600-LCMO) for the RMC structural modeling using neutron diffraction patterns and a neutron PDF of $\sum c_i c_j b_i b_j \{g_{ij}(r) - 1\}$ (c_i and b_i: concentration and coherent bound scattering length of atom i, and $g_{ij}(r)$: partial pair distribution function of atoms i and j, respectively). Initial structures were created in which each atom was randomly placed to match the Rietveld refinement results and reproduced by modeling. During modeling, simultaneous attempts were made to swap the metal atoms with the probabilities of 0.6 for the translation of the constituent atoms (Li, Cr, Mn, and O) and 0.2 for the swapping of Li and Cr as well Li and Mn. The particle sizes and morphologies of the obtained samples were observed using a scanning electron microscope (SEM; JEOL, JSM-7600F). The morphologies and surface conditions of the obtained particles were observed using a scanning/transmission electron microscope (JEOL JEM-ARM200F S/TEM with a Schottky field emission gun). This microscope was equipped with both probe and image correctors for high-resolution TEM observation. as Additionally, a JEM ARM200F STEM with a cold-field emission gun and a GIF Quantum ER EELS was utilized for STEM-EELS spectral imaging. Both microscopes were operated at an accelerating voltage of 200 kV. To investigate the structure change and oxidation state after charge–discharge reactions, the cathodes were carefully removed

from the cells after the charge–discharge reaction in the Ar-filled glove box, washed, and immersed in DMC overnight to remove the electrolyte. They were then dried and sealed in a laminate for Cr K-edge and Mn K-edge XANES or a transfer vessel for Cr L-edge, Mn L-edge, and O K-edge. The K-edge and L-edge XANES of each element in the electrodes after the charge–discharge reactions were measured at room temperature using synchrotron radiation at beamlines BL15 and BL12, respectively, of the Saga Light Source. XANES measurements for Cr, Mn L-edge, and O K-edge, which have a lower absorption energy, were carried out using the total electron yield method.

References

1 T. E. Faber, J. M. Ziman, *The Philosophical Magazine: A Journal of Theoretical Experimental and Applied Physics*, 1965, 11(109), 153–173.

2 K. Ohara, S. Tominaka, H. Yamada, M. Takahashi, H. Yamaguchi, F. Utsuno, T. Umeki, A. Yao, K. Nakada, M. Takemoto, et al., *J. Synchrot. Radiat.*, 2018, 25 (6), 1627–1633.

3 B. H. Toby, R. B. Von Dreele, *J. Appl. Cryst.*, 2013, 46, 544-549.

4 M. G. Tucker, D. A. Keen, M. T. Dove, A. L. Goodwin, Q. Hui, *J. Phys.: Condens. Matter*, 2007, 19, 335218-1-16.

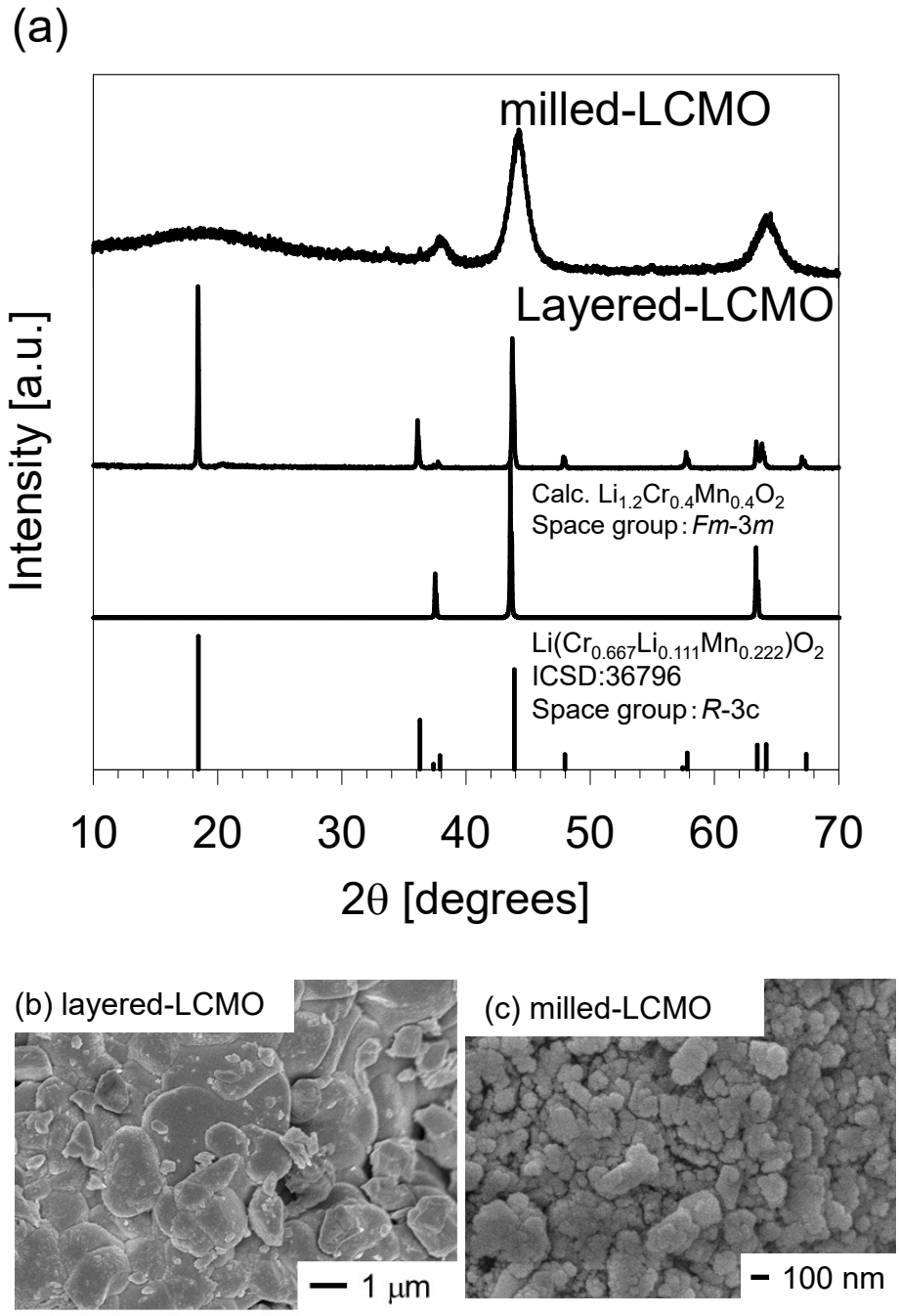

Figure S1 (a) XRD profiles, (b, c) SEM images for the obtained layered- and milled-LCMO.

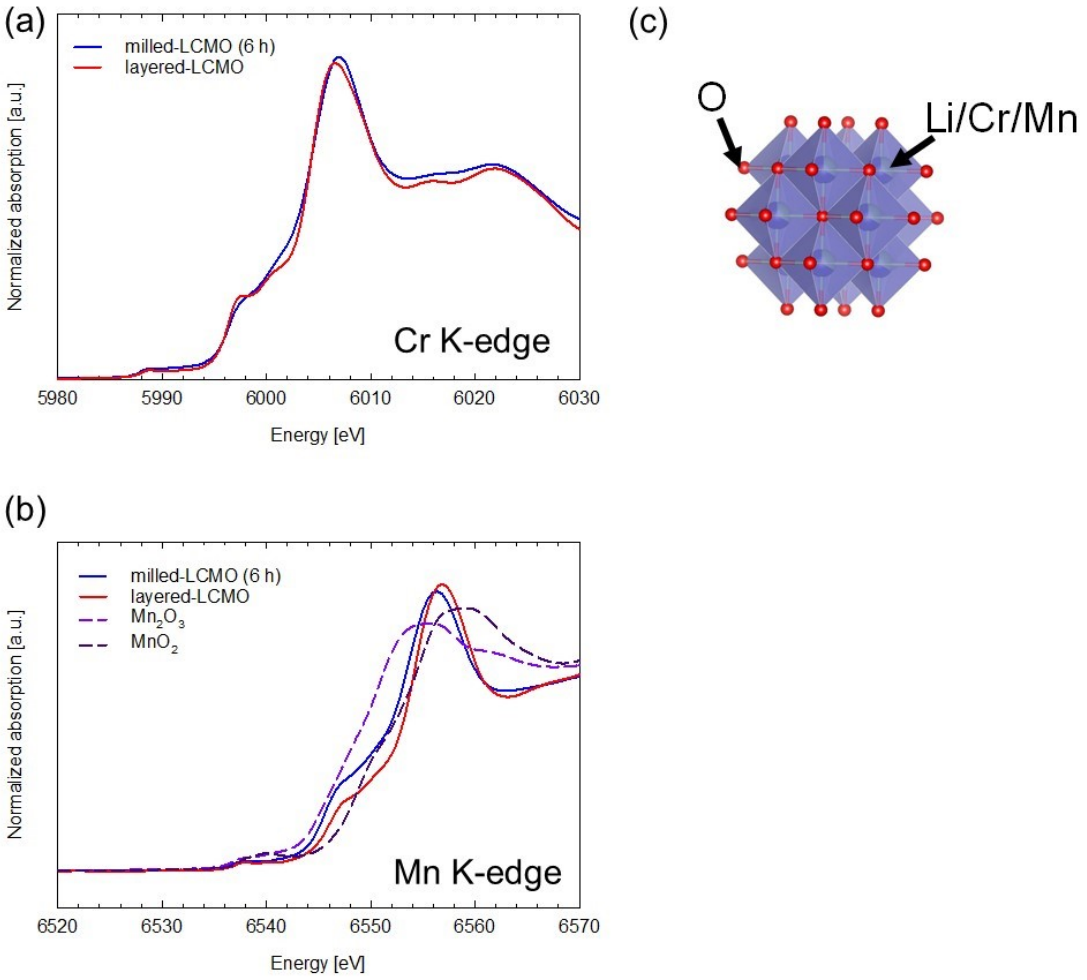

Figure S2 (a) Cr K-edge and (b) Mn K-edge XANES spectra for the obtained layered- and milled-LCMO. (c) The structure of the disordered rocksalt-type LCMO.

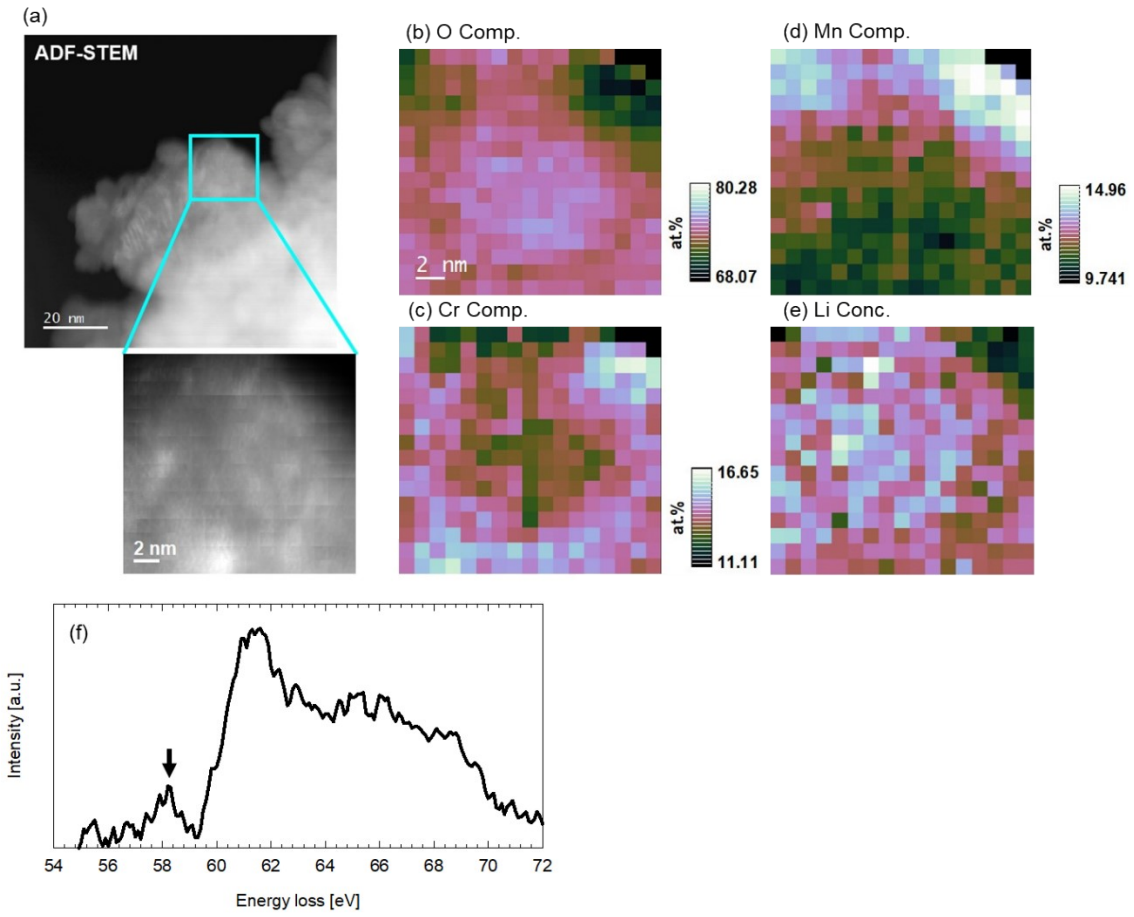

Figure S3 (a-e) Image diagrams based on STEM-EELS elemental mapping results and (f) Li K-edge EELS spectrum for milled-LCMO. The elemental distributions are normalized by the projected sample thickness to show the relative local concentrations.

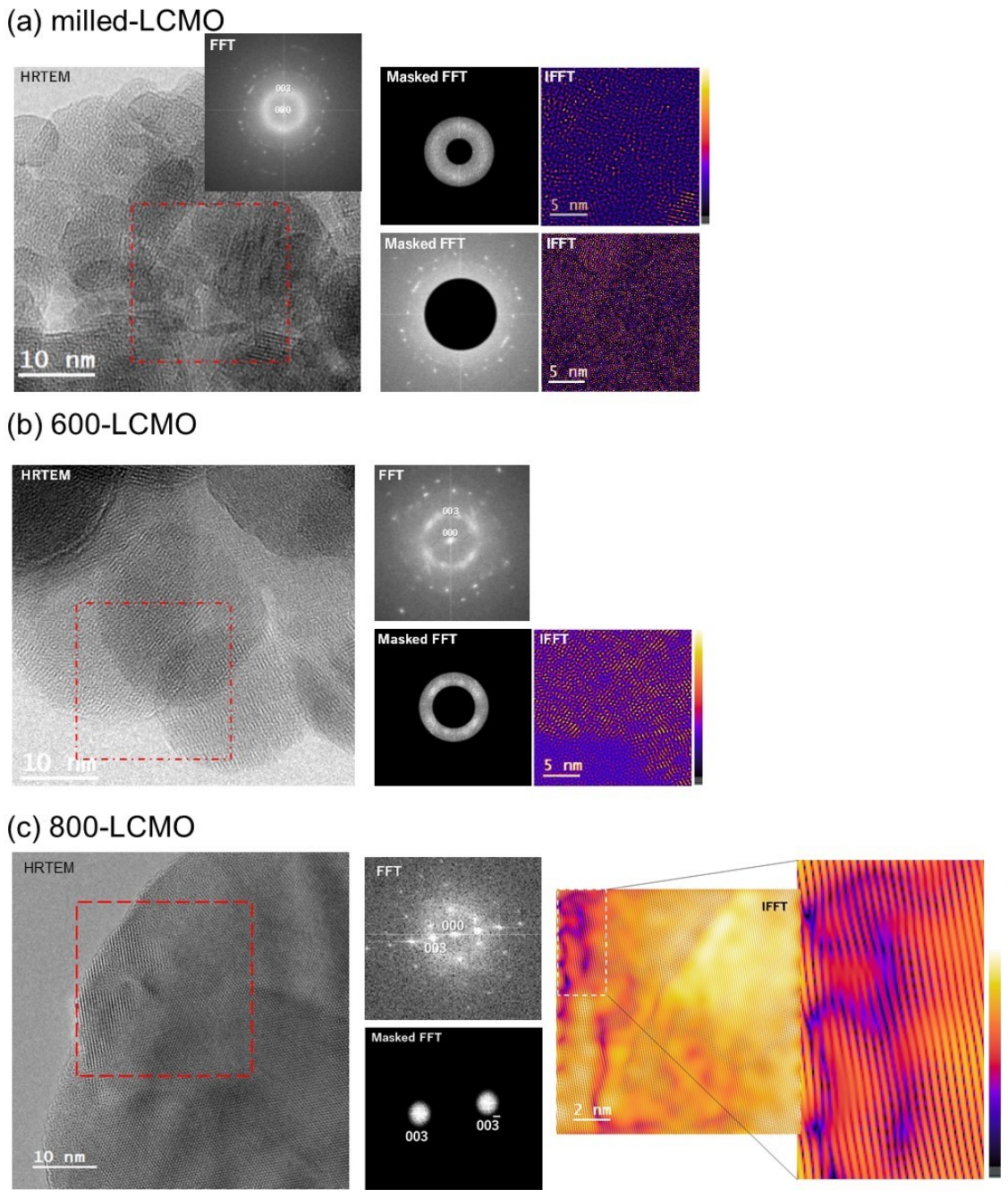

Figure S4 HRTEM image, FFT powerspectrum from framed area, and its inverse FFT image of masked FFT for (a) milled-LCMO, (b) 600-LCMO, and (c) 800-LCMO.

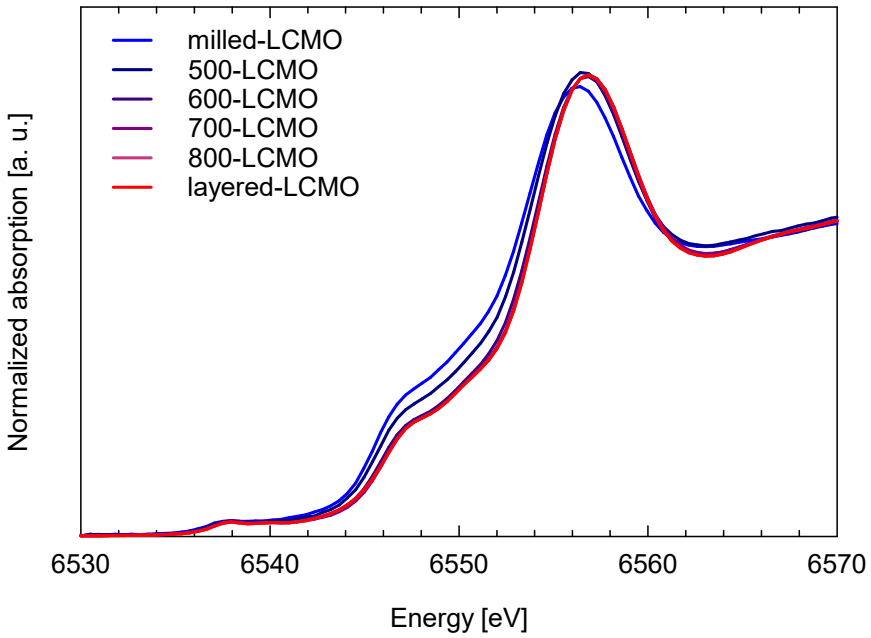

Figure S5 Mn K-edge XANES spectra for thermally treated LCMO at various temperatures.

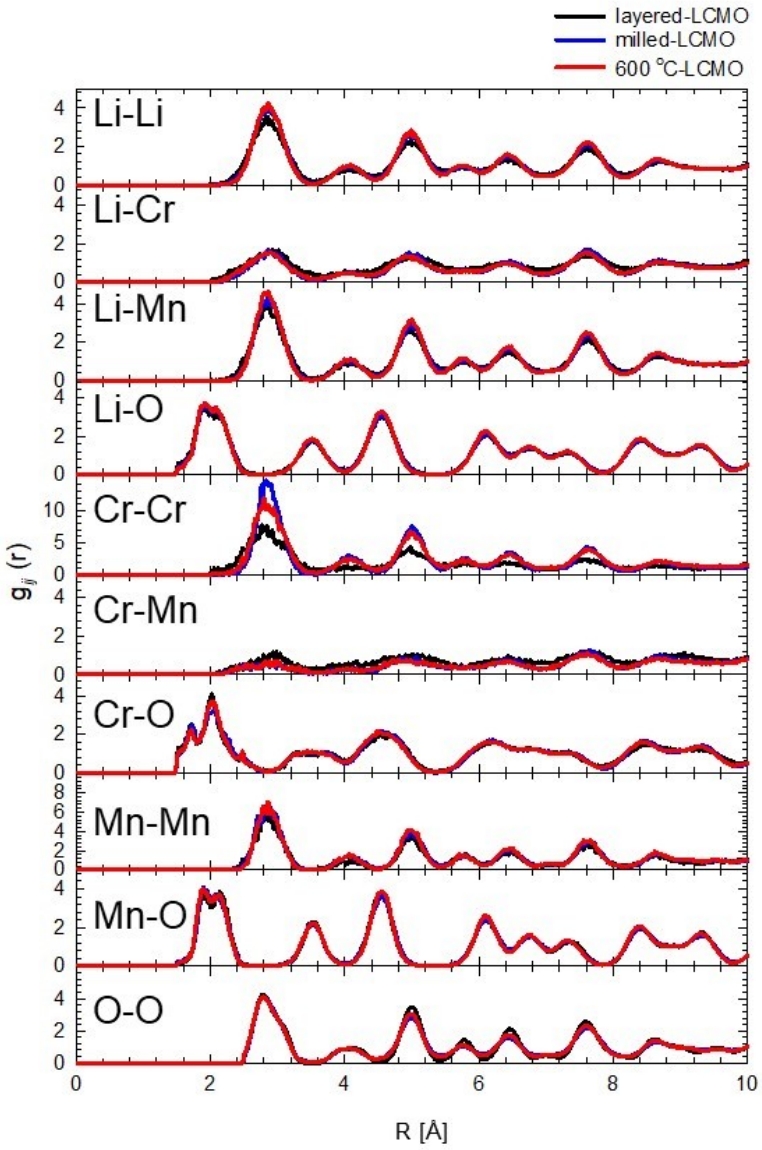

Figure S6 Partial pair distribution functions from the neutron diffraction of Li-Li, Li-Cr, Li-Mn, Li-O, Cr-Cr, Cr-Mn, Cr-O, Mn-Mn, Mn-O, and O-O correlations for layered-LCMO, milled-LCMO, and 600-LCMO powders.